

SHOCK PHYSICS DATA RECONSTRUCTION  
USING SUPPORT VECTOR REGRESSION

NIKITA A. SAKHANENKO\* and GEORGE F. LUGER†

Computer Science Department, University of New Mexico  
MSC 01 1130, 1 University of New Mexico  
Albuquerque, NM 87131, USA

\*sanik@cs.unm.edu

†luger@cs.unm.edu

HANNA E. MAKARUK‡, JOYSREE B. AUBREY§ and DAVID B. HOLTkamp¶

Physics Division, Los Alamos National Laboratory  
D 410 LANL, Los Alamos, NM 87545, USA

‡hanna\_m@lanl.gov

§jba@lanl.gov

¶dholbkamp@lanl.gov

Received 26 June 2006

Revised 31 July 2006

This paper considers a set of shock physics experiments that investigate how materials respond to the extremes of deformation, pressure, and temperature when exposed to shock waves. Due to the complexity and the cost of these tests, the available experimental data set is often very sparse. A support vector machine (SVM) technique for regression is used for data estimation of velocity measurements from the underlying experiments. Because of good generalization performance, the SVM method successfully interpolates the experimental data. The analysis of the resulting velocity surface provides more information on the physical phenomena of the experiment. Additionally, the estimated data can be used to identify outlier data sets, as well as to increase the understanding of the other data from the experiment.

Keywords: Support vector regression; data extrapolation; VISAR; shock waves; high explosive material damage and spall.

PACS Nos.: 62.50.+p, 07.05.Mh, 07.05.Kf, 68.18.Jk, 06.60.Jn.

## 1. Introduction

Experimental shock physics studies how materials behave under the extremes of deformation, pressure, and temperature, when shock waves interact with them.<sup>1</sup>

\*Corresponding author.

Most often these strong shock waves are produced by using high explosives or propellant guns. Many different diagnostic techniques<sup>2</sup> have been used to investigate material's response to extreme conditions.

Usually, experimental equipment is destroyed during the test due to the exposure to the shock waves. Because of this, experiments are sometimes quite expensive and complex. In order to conduct a thorough investigation of one physical property as a function of another, a number of experiments have to be repeated at significant cost and complexity. As the result, the data set available to a researcher is often very sparse: There may be a small number of experiments, or each experiment can be sampled with only a few diagnostics.

In this paper we apply a support vector machine (SVM) technique for regression to data estimation based on the velocity measurements from the underlying experiment. A Velocity Interferometer System for Any Reflector (VISAR) that provides the data for this work, records a point velocity of the moving surface after a tin sample is shocked with high explosives.<sup>3-5</sup> One can find a more detailed description elsewhere.<sup>6</sup> The VISAR data presented here describe the behavior of the free surface of the tin coupon under the effect of a high explosive (HE) generated shock wave. The analysis of the time dependence of the velocity magnitude can provide information on the yield strength of the material, and the thickness of the leading damaged layer that may separate from the bulk material during the shock/release of the sample.

The most common use of the SVM technology is for classification, though the SVM for regression data analysis, used in this paper, is a rapidly growing research area. Fields, in which SVM methods were successfully used, include geostatistics,<sup>7</sup> bioinformatics,<sup>8</sup> data mining,<sup>9</sup> forecasting,<sup>10</sup> and others. SVM methods have never been applied to VISAR data, nor to any shock physics data set. Vannerem et al.<sup>11</sup> attempted to analyze simulated high energy physics data using a support vector classification method. Another application of SVM in the analysis of physics data is presented by Cai et al.,<sup>12</sup> describing how the support vector machine is used to classify sonar signals. Although SVM for regression is rarely applied in physics, some successful support vector regression applications also exist. In civil engineering, Dibike et al.<sup>13</sup> showed how support vector regression techniques can be useful in the problem of stream flow data estimation based on records of rainfall and other climatic data.

In Sec. 2 we give a description of the underlying experiment and the way the data are captured. The problem definition — intuitive and formal — is given in Sec. 3. In Sec. 4 we define a support vector regression method and its advantages. The features of the data under consideration are given in Sec. 5. In Sec. 6 we analyse how support vector regression techniques are applied. Finally, we conclude in Sec. 7.

## 2. Underlying Experiment

### 2.1. Shock test overview

The data used in this paper are acquired from a set of experiments where a metal coupon is shocked by high explosives, detonated with a single point ignition. Using recorded data, researchers study the behavior of the damaged/melted metal sample. Figure 1 shows a schematic view of the initial experimental configuration.

A metal sample is placed on top of a 12.7 mm thick high explosive (HE) disc. The diameter of the cylindrically shaped sample is the same as that of the HE disc: 50.8 mm. In order to perform a symmetric single point ignition of the HE disc, a point detonator is attached to the center of the disk of HE. Note that the experimental setup is axially symmetric, which is important for reducing the complexity of further data analysis and providing more intuition about physical phenomena in the experiment.

A VISAR probe is pointed at the center of the metal sample. During the experiment the probe transmits a laser beam at the top surface of the shocked metal, and the velocity of this surface is deduced from the Doppler shifted light reflected from it (see the next section for more details). As a result, the time series of the velocity is recorded during the experiment.

During the same experiment a proton beam is incident perpendicular to the axis of symmetry. A series of Proton Radiography (pRad) images captures the current state of the experiment in a series of time steps produced by the focussed proton beam. PRad imagery is a tomography technique, thus it can be compared to X-ray

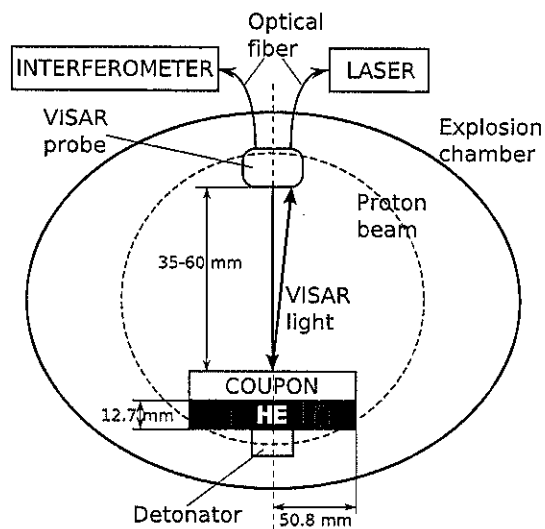


Fig. 1. A schematic illustration of the setup of the underlying experiment and its connection with the VISAR system.

or gamma ray tomography. Since a pRad image exposure time is less than 50 ns, this technique is more suitable for recording ultra fast experiments, e.g., up to 20 images are taken in a single experiment, such as the one described in this paper. Another advantage of the pRad technique is that a proton beam penetrates metal fragments without heavy attenuation, which is typical for an X-ray beam. In this paper we focus on VISAR data analysis, whereas other publications<sup>6</sup> provide more details about pRad imagery analysis.

In order to identify the changes in physical processes over a set of experiments, two parameters of the initial experiment setup are varied between different experiments. These parameters are the thickness of a metal coupon and the type of the metal. For simplicity of this paper, we consider only those experiments that are performed on tin samples of several selected thicknesses.

## 2.2. Capturing velocity with VISAR

A Velocity Interferometer System for Any Reflector (VISAR) is a system that captures changes of the velocity of a moving surface by measuring the Doppler shift of a laser beam reflected from the surface. Velocity changes as small as a few meters per second can be detected by the VISAR system.

The general components of a VISAR system, such as lasers, detectors, and optical elements, are shown in Fig. 1. The laser emits a beam, which is delivered to the VISAR probe via fiber-optic cables. If the probe is properly focussed, some of the laser light reflects from the moving surface and gets back into the probe. After that the captured reflected light is forwarded to the interferometer. Since the reflected light is Doppler shifted, the interferometer is able to determine the velocity of the moving surface.

Once the Doppler shifted light is captured by the probe it is transmitted to the interferometer, shown in Fig. 2, where it is split into two beams. Using optics, one

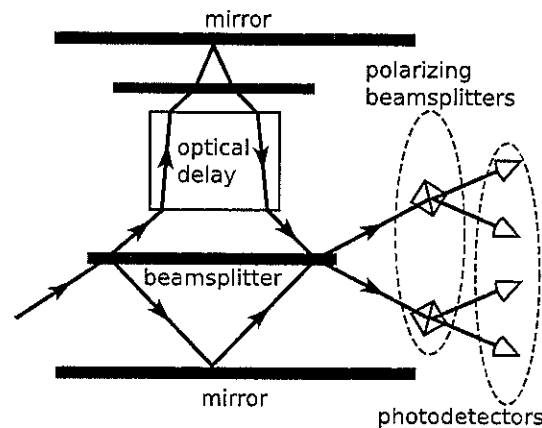


Fig. 2. A schematic illustration of the interferometer subsystem used in the VISAR system.

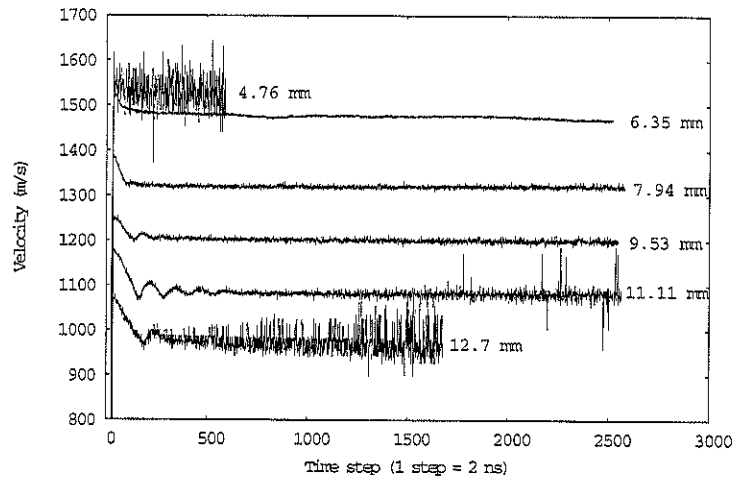


Fig. 3. Velocities recorded by the VISAR system from the experiments on tin coupons with different thicknesses (from 4.76 mm to 12.7 mm).

of the signals is delayed, hence the signals cover different distances. After that the signals are adjusted so as to make them interfere before they reach the photodetectors. The final VISAR information is retrieved from the system by recording the intensity signals from the photodetectors. More details about the VISAR system and its operation can be found elsewhere.<sup>3-5</sup>

Figure 3 shows different time series data produced by the VISAR system after several experiments. The output of a VISAR system agrees well ( $\sim 1\%$ ) with velocity results obtained from analyzing the locations of different visible fragments of a pRad image and calculating their corresponding velocities.<sup>14</sup>

### 3. Problem Definition

Due to the high cost of the experiments and their complexity, the amount of the experimental data obtained is limited. Given these limitations, this paper attempts to tackle the problem of measurements estimation for the missing experiments, or for those experiments whose VISAR data recordings were not successful, although other components of the data, such as pRad images, were recorded correctly. This can potentially allow for a successful interpretation of an experiment, despite errors in the VISAR data recording, and avoiding the need for repeating the experiment. One might notice that this problem is strongly connected to the detection of “outlier” experiments: those experiments that due to the errors in the initial setup or for some other reasons went wrong. The experimental data that do not “fit” with other “good” experiments can be identified by data estimation techniques. Using data computed by estimation techniques, we can increase the informational output of VISAR and overcome the scarcity of the experiments. Researchers want to understand all the phenomena of these experiments, hence using the combination of

the VISAR data with the data estimations provides more possibilities for better perception of physical processes than using the VISAR data alone.

In addition, velocity estimations can be compared with different kinds of hydrocode models, simulating an experiment under relevant physical laws defined by a set of physical equations. The initial conditions of a hydrocode simulation are identical to those of the real experiment. Depending on the type of a hydrocode, the simulations (frequently called *numerical experiments*) are conducted in two- or three-dimensional spaces.

Furthermore, velocity estimations can be used to support and even improve other types of data. The pRad imagery, which is collected during these experiments, is one such type of data.

### 3.1. Formal problem

Since each VISAR data point (in a time series that may extend over several microseconds) is a tuple  $(\text{time}, \text{thick}, \text{vel})$  ( $\text{time}$  is the time when the recording took place,  $\text{thick}$  is the thickness of the coupon in the experiment, and  $\text{vel}$  is the recorded velocity), the data form a two-dimensional surface in the three-dimensional space. Thus, to deal with the problems identified above, we need to reconstruct the two-dimensional surface using the VISAR data sets.

Mathematically speaking, the problem is to find a regression of velocity on the thickness of a sample and time. That is, given three random variables  $T, V, W$  corresponding to  $\text{time}$ ,  $\text{velocity}$ , and  $\text{thickness}$  that map a probability space  $(\Omega, A, P)$  into a measure space  $(\Gamma, S)$ , we want to estimate coefficients  $\lambda$  from some set  $\Lambda \subseteq \Gamma$  such that the error  $e = V - \eta(T, W; \lambda)$  is small, where  $\eta : \Gamma^2 \times \Lambda \rightarrow \Gamma$  is a regression function. Note that most of the time, including the case considered in this article,  $\Gamma = \mathbb{R}$ . The variable  $V$ , the regression of which we try to find, is called an *observation*. The variables  $T, W$ , upon which the regression is based, are called *regression factors*.

## 4. Support Vector Regression

### 4.1. Definition

The Support Vector Machine (SVM)<sup>15</sup> belongs to the so called *supervised learning* methods, and like a majority of them needs to be trained using a data set of  $k$  points  $\{(x_i, y_i) | x_i \in X, y_i \in Y, i = 1 \dots k\}$ . The SVM method estimates a functional input/output relationship from this set, assuming that each training data point is randomly generated by an unknown function  $f$ :

$$f(x) = w \cdot \phi(x) + b. \quad (1)$$

Here  $\phi$  is a nonlinear mapping  $\phi : X \rightarrow H$  from an input space  $X \subseteq \mathbb{R}^n$  to a high-dimensional feature space  $H$ . The parameter  $b$  belongs to an output space  $Y \subseteq \mathbb{R}$ ,

and  $w \in H$ . These parameters are obtained by minimizing the regularized risk<sup>15</sup>

$$R = \sum_{i=1}^k L(f(x_i), y_i) + \lambda \|w\|^2,$$

that consists of an empirical risk (the first term) and a regularization term (the second term). The regularization term is defined in such a way that the estimated function  $f$  is flat. We use  $\varepsilon$ -intensive loss function<sup>16</sup> as a model for an empirical risk. The loss function is

$$L(f(x), y) = \begin{cases} |f(x) - y| - \varepsilon, & \text{if } |f(x) - y| \geq \varepsilon \\ 0, & \text{otherwise} \end{cases}.$$

Besides being a supervised learning method, SVM is a kernel method. A kernel  $K$  of a function  $h : A \rightarrow B$  defines an equivalence relation on  $A$  as follows

$$K(h) = \{(a_1, a_2) | a_1, a_2 \in A, h(a_1) = h(a_2)\} \subseteq A \times A.$$

Classification problems were among the first applications of SVM. In order to classify the data, the algorithm transforms the feature space  $H$ . It then attempts to find a hyperplane in the new space that separates the data into two classes such that the distance between the classes and the plane is maximal. Later the SVM technique was successfully used for regression estimation (Support Vector Regression, SVR). SVR produces a model based on only a subset of training data, since the loss function used during training of SVR ignores all the data points that are close to the model prediction.

#### 4.2. SVR advantages

There are several attractive features of the SVM approach<sup>17</sup> that were decisive when we chose this method for addressing our problem.

- **Good generalization performance**

One attractive feature is the good generalization performance. A unique principle of structural risk minimization<sup>18</sup> is the key to such generalization achievement of the SVM method.

- **Sparse representation**

A solution obtained by SVM depends only on a subset of the training data, called support vectors. This is why the representation of the solution is sparse.

- **No local minima problem**

Since training of the SVM is equivalent to solving a linearly constrained quadratic programming problem, its solution is unique and globally optimal. Therefore, we do not need to worry about local minima.

- **Kernel power**

The involvement of kernels in the SVM technique allows us to work with arbitrarily large feature spaces: there is no need to explicitly compute  $\phi$  — the

mapping from the data space to the feature space, thus avoiding computing the dot product of (1).

It is known<sup>19</sup> that a linear algorithm that uses only dot products can be transformed to a nonlinear one by replacing all the dot products with a kernel function. Note that although the SVM algorithm after the kernel transformation is nonlinear, it is still linear in the feature space (the range of the mapping  $\phi$ ). Since when using the SVM algorithm we apply a kernel instead of  $w \cdot \phi(x)$  of (1), the explicit computation of  $\phi$  is not needed. This kernel transformation of a linear algorithm to a nonlinear one is known as the *kernel trick*.<sup>19</sup>

### 5. Features of VISAR Velocity

The VISAR data we use in this paper are suitable for application of supervised learning methods, since the VISAR system captures values of some unknown function for each given couple (time, thickness). Hence the support vector regression method can be also applied to this task, using the velocity component of each data point as a target value and the pair of time and thickness components as feature values. Unfortunately, we cannot apply SVR in a straight forward manner, due to different features of the VISAR data.

Figure 4(a) presents the entire VISAR data set. As can be seen in the figure, the data is considerably extended along the time axis. The reason for this is the fact that the available data set consists of the time series of velocities corresponding to each experiment included in the set. Recall that throughout each experiment the VISAR system measured the velocity of the moving surface every 2 ns for up to 6000 time steps. Note however that in some experiments the VISAR recordings stop having useful information (due to high noise and artifacts) earlier than in others. This happens because the experiments on thinner samples produce a more diffuse moving surface, velocity of which is harder for the VISAR system to capture, than a moving surface in the experiments on thicker samples. It has been identified experimentally

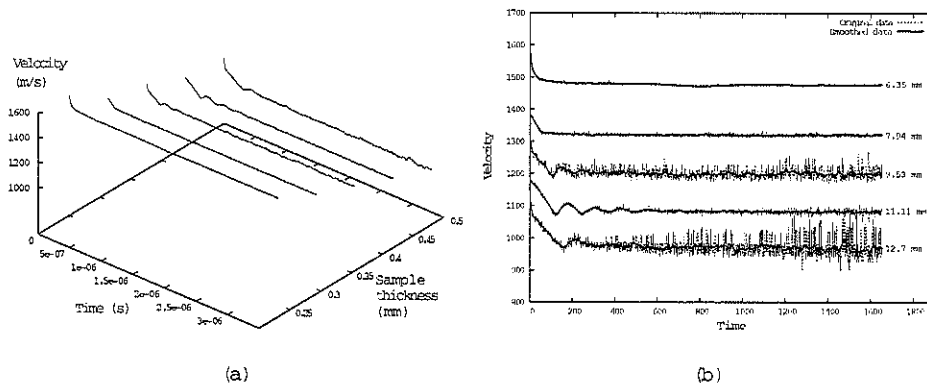


Fig. 4. The available VISAR data set: (a) in three-dimensional Time  $\times$  Thickness  $\times$  Velocity data space; (b) projected on the Time  $\times$  Velocity plane together with its smoothed version.



that SVR performs better on the aligned data; this is why we cropped the data by the shortest sequence (1656 time steps). Along the thickness axis the data spans the thicknesses starting from 6.35 mm up to 12.7 mm with 1.5875 mm step. After cropping the time series, the data used by the SVM method is combined of 5 time series with 1656 points each.

Since for different experiments the start of a test (first motion of the tin surface) and the time step at which the measurements were recorded were different, the output data have to be time-aligned. The goal of the alignment is to make each time series start exactly at the moment when the shock wave reaches the top surface of the coupon bringing the surface to motion. Figure 4(b) shows the projection of the complete data set on the  $T \times V$  plane. The abscissa of this figure shows the amount of time steps, 2 ns each. The dashed lines represent the original time series, whereas the solid lines show these data after smoothing with a triangular window.

Note also that the magnitudes of the components' values of each data point (time, thickness, and velocity) are of the drastically different order. The order of magnitude of the time component is  $10^{-6}$ , whereas it is 1 for the thickness component, and  $10^3$  for the velocity component.

In the next section we show how to deal with the data features of the VISAR measurements identified above. We also show how to find the optimal SVM configuration for the best application.

## 6. The use of Support Vector Regression Techniques

The quality of the resulting regression is affected by several factors. The main one is the error in the VISAR data that could be the result of tiny misalignments in the initial experimental setup or other hard-to-control problems during the experiment. This error together with the error contributed during the data preprocessing affects the accuracy of the reconstructed surface the most. It is calculated that a VISAR system measures the velocity values with an absolute error of 3–5%. This error is an approximation computed from differences between repeated experiments. Despite a very small number of repeated experiments which do not support a more robust statistical analysis, this level of uncertainty is in the range of values generally accepted by VISAR experimenters.<sup>3–5</sup> This error together with the noise and a potential inaccuracy caused by the time alignment of the SVR input data transfers into the regression result.

The specific features of the VISAR data outlined in the previous section also affect the accuracy of the reconstructed surface. Recall that the time series recorded in various experiments have different length. Since it was observed that the SVM performance improves considerably if the data is aligned, we cut the data by the shortest time series. Scaling data, coordinates of which are of significantly different orders of magnitude, also improves the SVM performance.

The application of SVR to the data at this point (the data that have been time-aligned, cropped, and scaled) yields overfitted results. For any interval there are more data points along the time axis than those along the thickness axis, because the distance between two neighbor points in the time direction is much smaller than in the thickness direction. In our research we dealt with the overfitting problem by transforming the data in a custom manner such that the interval between any two neighbor points is one unit long in any direction.

It is known that SVM with nonlinear kernels performs better when the dynamics of an underlying experiment are nonlinear. Among nonlinear kernels, the Gaussian Radial Basis Function (RBF) kernel shows good results under the general smoothness assumption.<sup>20</sup> Furthermore, as practice showed, the SVR method with a simpler than RBF kernel, e.g., a polynomial kernel, trains slower and returns non-satisfactory results. This is why we chose the Gaussian RBF

$$k(x, y) = e^{-\gamma \|x-y\|^2}$$

as a kernel for the estimation of a velocity surface.

There are three free parameters in the SVR method with an RBF kernel that directly influence its execution. These parameters are the RBF radius  $\gamma$ , the size  $\varepsilon$  of the error-insensitive zone, also known as an  $\varepsilon$ -margin or an  $\varepsilon$ -tube, and the regularization constant  $C$ , also called a capacity factor or an upper bound on the Lagrangian multipliers. Recall that  $\varepsilon$  determines the amount by which a training point is permitted to diverge from the regression, which directly affects the accuracy of the regression.

In order to identify the optimal values of the free parameters that lead to the best application of the SVR method to the VISAR data, we use standard  $k$ -fold cross-validation. After dividing the data set into  $k$  parts, we used  $k - 1$  parts for training the supervised learning machine and the remaining part for its successive validation. This process is repeated  $k$  times using each part only once for validation. At the end of each cross-validation we computed an  $l^2$  error corresponding to a particular instantiation of the SVR free parameters. The error changes as a function of the values of these parameters as shown in Fig. 5.

From Fig. 5 we can study the relationship between the free parameters and the error. For example, we can see that if  $\varepsilon$  and/or  $\gamma$  increases, then the error also grows. Note also that the regularization constant  $C$  influences the error the most when the radius  $\gamma$  is the smallest. This influence of  $C$  on the error reduces as  $\gamma$  grows, becoming negligible when  $\gamma$  exceeds 0.3. Furthermore, given a small  $\gamma$ , parameter  $C$  changes the error more with a smaller  $\varepsilon$ . Finally, after analyzing the error we identified that it is the smallest when the tuple  $(\varepsilon, \gamma, C)$  is in the range  $[(0.001, 0.1, 0.75) \dots (0.001, 0.1, 1.0)]$ . Note that this range provides suboptimal parameter values. In order to identify a final model that produces the most accurate velocity surface, expert knowledge was used, i.e., an expert from the physics domain chose the best surface out of several produced by models with different suboptimal

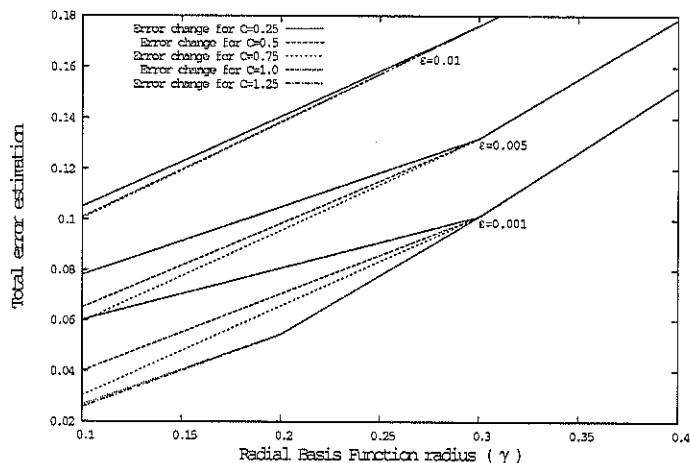


Fig. 5. The dependence of the error on the SVM free parameters.

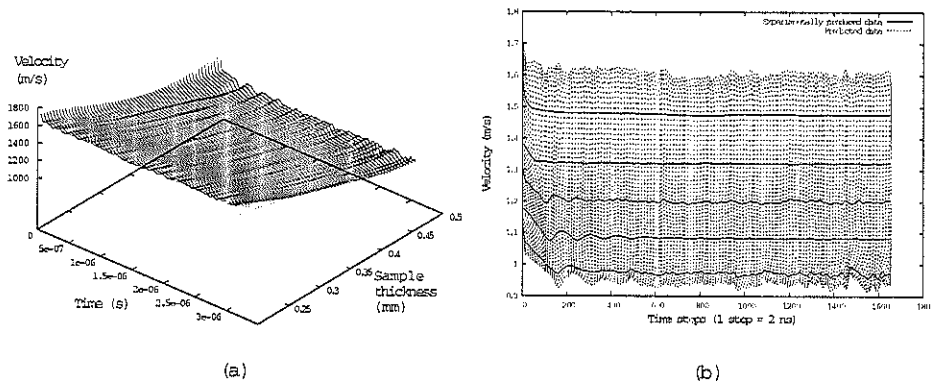


Fig. 6. Prediction results of the SVR method: (a) in three-dimensional Time  $\times$  Thickness  $\times$  Velocity data space; (b) projected on the Time  $\times$  Velocity plane, the solid lines represent experimentally produced data and the dashed lines show the estimated data.

values. Fig. 6 shows the velocity surface (represented by the dashed lines) estimated by the SVR method from the given data (showed with the solid lines).

A velocity value for any (time, thickness) pair can be easily estimated, once the velocity surface is found. We can also identify the potentially failed VISAR data that veers significantly from the surface, assuming that the reconstructed surface is sufficiently accurate. Much more information about the velocity changes is provided by the estimated surface together with VISAR readings than from the experimental data alone. For an experiment, in which only pRad data were successfully recorded, the surface can provide a velocity time series, enhancing the analysis quality of the experiment. This, in turn, helps researchers to understand the entire physical system better.

Note that in this paper we used the SVM-light implementation of the SVR method.<sup>21</sup>

## 7. Conclusions and Future Work

An interesting case of VISAR data analysis was discussed in this paper. We sought to estimate the velocity values between the data points recorded by the VISAR system. Using the support vector regression method, we successfully reconstructed the two-dimensional velocity surface in the three-dimensional data space with Time, Thickness, and Velocity as its dimensions. In order to find the optimal values of the SVR free parameters, a grid search as well as expert knowledge were used. Support vector regression does not require a large input data set for producing good results. This is very helpful in the environment of expensive and highly complex experiments providing a limited amount of data points.

The velocity surface delivers a lot of information about the patterns of the velocity as a function of time and thickness, more than sparse experimentally obtained VISAR data alone. PRad imagery analysis, hydrocode simulations, and other areas of analysis of shock physics experiments may also benefit from the VISAR data enhanced by the velocity estimations. Moreover, the “outlier” experiments, those tests that for some reason went wrong, can be identified more easily with the help of the reconstructed velocity surface. The data from an “outlier” experiment will be substantially different than the data predicted by the surface.

This work can be advanced in several directions, one is to determine a better way for finding optimal values for the SVM free parameters. Recall that a grid search and expert knowledge were used, leading to the suboptimal parameter values. It might be very useful to design an online learning algorithm for SVM parameter fitting specific to the VISAR data. The usage of a custom kernel instead of an RBF is another direction of further research. Intuitively, the results of support vector regression may be improved by using an elliptical kernel that takes into account the data density along one axis and the data sparsity along the other axis. Another direction for future work might be to attempt to capture uncertainty in the surface reconstruction. Currently, SVR returns a point estimate, however it is more appealing to find a conditional distribution of the target values given the feature values. Such methods as relevance vector machines, Bayesian SVM, and other extensions of the original SVM method that employ probabilistic methods might provide considerably more information about the underlying experiments.

## Acknowledgments

The authors thank Brendt Wohlberg for numerous thought-provoking discussions about SVM applications. We also thank David A. Clark, Dale Tupa, and Brian Hollander for assistance in taking the VISAR data. This work was supported by the Department of Energy under the ADAPT program.

## References

1. Ya. B. Zel'dovich, *Physics of Shock Waves and High-Temperature Hydrodynamic Phenomena* (Dover Publications, Mineola, NY, 2002).
2. W. M. Isbell, *Shock Waves: Measuring the Dynamic Response of Materials* (Imperial College Press, London, 2005).
3. L. M. Barker and R. E. Hollenback, *J. Appl. Phys.* 43, 4669 (1972).
4. L. M. Barker and K. W. Schuler, *J. Appl. Phys.* 45, 3692 (1974).
5. W. F. Hamming, *Rev. Sci. Instrum.* 50, 73 (1979).
6. D. B. Holtkamp et al., *A Survey of High Explosive-Induced Damage and Spall in Selected Materials Using Proton Radiography* – Proc. Shock Compression of Condensed Matter, AIP Conference Proceedings, Vol. 706, eds. M. D. Furnish et al. (AIP, 2003), p. 477.
7. M. Kanevski, M. Maiguan and A. Pozdnukhov, *Active Learning of Environmental Data Using Support Vector Machines* – Proc. Conference of International Association for Mathematical Geology, IAMG Conference Proceedings (To be published, 2005).
8. H. Rangwala and G. Karaypis, *Bioinformatics* 21, 4239 (2005).
9. B. Schölkopf, C. Burges and V. Vapnik, *Extracting Support Data for a given Task* – Proc. First International Conference on Knowledge Discovery and Data Mining, eds. U. M. Fayyad and R. Uthurusamy (AAAI Press, 1995).
10. L. J. Cao and F. E. H. Tay, *IEEE Transactions on Neural Networks* 14, 1506 (2003).
11. P. Vannerem, K.-R. Müller, B. Schölkopf, A. Smola and S. Sölkner-Renbold, *Classifying LEP Data with Support Vector Algorithms* – Proc. 6th Int. Workshop on New Computing Techniques in Physics Research (IHENP 99) (To be published, 1999).
12. C.-Z. Cai, W.-L. Wang and Y.-Z. Chen, *Int. J. Mod. Phys. C* 14, 575 (2003).
13. Y. B. Doble, S. Velickov, D. Solmatine and M. B. Abbott, *J. Comput. Civil Eng.* 15, 208 (2001).
14. H. E. Mamanuk, N. A. Sakhanenko and D. Holtkamp, *Analysis of Proton Radiography Images of Shock Melted/Damaged Tin*, LANL Tech. Report, LA-UR-06-107, 2006.
15. B. Schölkopf and A. Smola, *Learning with Kernels. Support Vector Machines, Regularization, Optimization, and Beyond* (MIT Press, 2001).
16. V. Vapnik, *The Nature of Statistical Learning Theory* (Springer, 1999).
17. J. Shawe-Taylor and N. Cristianini, *Kernel Methods for Pattern Analysis* (Cambridge University Press, 2004).
18. V. Vapnik, *Estimation of Dependences Based on Empirical Data* (Springer-Verlag, New York, 1982).
19. M. Aizenman, E. Braverman and L. Rozonoer, *Automation and Remote Control* 25, 821 (1964).
20. A. Smola, B. Schölkopf and K.-R. Müller, *Neural Networks* 11, 637 (1998).
21. T. Joachims, *Making large-scale SVM learning practical*, *Advances in Kernel Methods – Support Vector Learning*, eds. B. Schölkopf et al. (MIT Press, 1999).